

Amorphization of Cu nanoparticles: Effects on surface plasmon resonance

H. Amekura, B. Johannessen, D. J. Sprouster, and M. C. Ridgway

Citation: *Appl. Phys. Lett.* **99**, 043102 (2011); doi: 10.1063/1.3615307

View online: <http://dx.doi.org/10.1063/1.3615307>

View Table of Contents: <http://apl.aip.org/resource/1/APPLAB/v99/i4>

Published by the [American Institute of Physics](#).

Related Articles

Downconversion from visible to near infrared through multi-wavelength excitation in Er³⁺/Yb³⁺ co-doped NaYF₄ nanocrystals

J. Appl. Phys. **110**, 113113 (2011)

High-Q optomechanical GaAs nanomembranes

Appl. Phys. Lett. **99**, 243102 (2011)

Faraday rotation enhancement of gold coated Fe₂O₃ nanoparticles: Comparison of experiment and theory

J. Chem. Phys. **135**, 224502 (2011)

Ionodeterioration of the silicon nanocrystal photoluminescence

J. Appl. Phys. **110**, 114904 (2011)

Metal nanoparticles in a photovoltaic cell: Effect of metallic loss

AIP Advances **1**, 042154 (2011)

Additional information on *Appl. Phys. Lett.*

Journal Homepage: <http://apl.aip.org/>

Journal Information: http://apl.aip.org/about/about_the_journal

Top downloads: http://apl.aip.org/features/most_downloaded

Information for Authors: <http://apl.aip.org/authors>

ADVERTISEMENT



AIPAdvances

Submit Now

Explore AIP's new
open-access journal

- Article-level metrics now available
- Join the conversation! Rate & comment on articles

Amorphization of Cu nanoparticles: Effects on surface plasmon resonance

H. Amekura,^{1,a)} B. Johannessen,² D. J. Sprouster,³ and M. C. Ridgway³

¹National Institute for Materials Science (NIMS), Tsukuba, Ibaraki 305-0003, Japan

²Australian Synchrotron, Clayton, VIC 3168, Australia

³Australian National University, Canberra, ACT 0200, Australia

(Received 9 May 2011; accepted 2 July 2011; published online 25 July 2011)

Crystalline copper nanoparticles (NPs) were formed in silica by multi-energy MeV ion implantations and then transformed to amorphous NPs by irradiation with 5 MeV Sn³⁺ ions. Optical absorption spectra of both the phases were evaluated in the ultra-violet to near-infrared regions. Compared with corresponding crystalline NPs of the same mean diameter, the amorphous NPs showed a low-energy shift of the surface plasmon resonance around 2.2 eV and less prominent absorption structure around 4 eV. These differences are explained by a strongly reduced electron mean-free-path in the amorphous NPs due to the loss of lattice periodicity. © 2011 American Institute of Physics. [doi:10.1063/1.3615307]

Surface plasmon resonance (SPR) of metal nanoparticles (NPs) has been subjected to extensive investigations aiming at applications to ultra-fast optical nonlinear devices,¹ one-molecule detection by enhanced Raman spectroscopy,² plasmonics,³ etc. While more than two thirds of the elements in the periodic table are metals, only NPs of very limited species, such as noble-metals and some exceptions, show a pronounced SPR simultaneously with chemical stability for practical applications. If amorphization preserves the pronounced SPR which is observed in the crystalline NPs of the same material, the number of the NP species showing a pronounced SPR increases in a single bound. Furthermore, the amorphization can be a new parameter controlling the SPR.

Because of the direction-insensitive nature of metal bondings, metals generally have structural flexibility against randomness introduced in the crystalline structures.⁴ This is in contrast with tetrahedrally bonded semiconductors, e.g., Si, Ge, etc, where the direction-sensitive bondings are weak against structural randomness. Consequently, semiconductors more easily suffer amorphization of their crystalline structures. Contrary, amorphous *bulk* metals which consist of *only one element* have never been successfully formed to date. While amorphous *alloy* metals in bulk form have been synthesized, the amorphous alloys consist of multi-elements, and in the most of the cases, they include a non-metallic element. In the form of thin films, past literature reported the formation of amorphous *elemental* metals of Fe (Ref. 5) by sonochemical processing. However, the amorphization was confirmed only by the disappearance of the x-ray diffraction (XRD) peaks and any information of the short-range order obtained by, e.g., the extended x-ray absorption fine structure (EXAFS) was not provided. It should be noted that XRD is not a powerful tool for determining whether a material is amorphous or nano-crystalline due to the extreme broadening of Bragg peaks with both decreasing crystal size and increasing amorphous fraction. Using vapor condensation at sub 20 K,⁶ an amorphous Co film of ~5 nm thick was

formed and the short-range order was evaluated at the same temperature by EXAFS. The EXAFS results were consistent with amorphization. However, the amorphous Co films were sensitive to temperature and re-crystallized much lower than room temperature (at around 120 K).

Ion irradiation has been recognized as an established technique to induce amorphization, mainly in semiconductors. If this technique also applies to metals, even in the form of thin film or nanostructures, various technologically relevant applications would be expected. Johannessen *et al.* have succeeded in the amorphization of Cu-NPs (Ref. 7) and Co-NPs (Ref. 8) embedded in thermally-oxidized SiO₂ layers and have studied their structural properties using synchrotron based x-ray techniques such as x-ray absorption spectroscopy (XAS) and small angle x-ray scattering (SAXS). In this letter, optical absorption spectra of the amorphous Cu NPs in the ultra-violet (UV), visible (Vis), and near-infrared (NIR) are described in order to understand the nature of the SPR of amorphous NPs.

Since the amorphization of Cu NPs is very sensitive to the fabrication parameters, we followed the recipe given by Johannessen *et al.*⁷ Silica glasses of KU-1 type (OH ~ 820 ppm) were implanted at liquid nitrogen temperature (LNT) with Cu ions of four different energies of 0.7, 0.9, 1.2, and 1.5 MeV up to respective fluences of 2.1, 4.2, 5.2, 7.2 × 10¹⁶ ions/cm² in order to obtain a nearly-flat concentration profile of ~3.6 at.% over a depth range of 0.6–1.0 μm.⁷ The samples were subsequently evaluated by EXAFS and the UV-Vis-NIR absorption measurements. The EXAFS spectra were taken in fluorescence mode at 12 K at the Cu K-edge at the Australian Synchrotron facility. The Fourier transformation was carried out on the *k*³-weighted spectra. All the EXAFS results are non-phase-corrected. The results are shown in Fig. 1(a). UV-Vis-NIR absorption spectra were determined in the wavelength range of 190–1700 nm from optical transmittance and reflectance spectra with a correction for multiple reflections in the samples. The details of the method were described in Ref. 9. The results are shown in Fig. 1(b).

In the as-implanted state, the EXAFS result (curve (i) in Fig. 1(a)) at the Cu edge shows only a strong peak around

^{a)}Author to whom correspondence should be addressed. Electronic mail: amekura.hiroshi@nims.go.jp. Tel.: +81-29-863-5477. Fax: +81-29-863-5599.

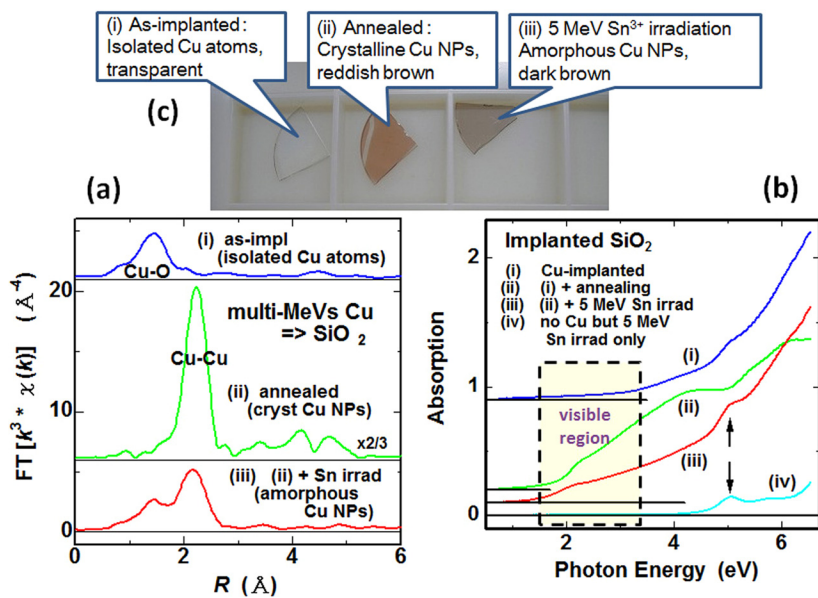


FIG. 1. (Color online) (a) Fourier transformed magnitude of k^3 -weighted EXAFS data at the Cu K -edge, from Cu-implanted silica (i) in as-implanted state, (ii) after annealing in forming gas, and (iii) after additional irradiation of 5 MeV Sn^{3+} ions. (b) Optical absorption spectra of Cu-implanted silica in the conditions (i), (ii), and (iii). The curve (iv) shows a spectrum from virgin silica irradiated with 5 MeV Sn^{3+} ions. (c) Photo-images of Cu-implanted silica in the conditions (i), (ii), and (iii). In panels (a) and (b), the curves are offset vertically for clarity and the horizontal lines indicate the corresponding baselines.

1.45 Å and no peak around 2.2 Å, which correspond to Cu–O and Cu–Cu distances, respectively. This indicates that each Cu atom is surrounded by O atoms; i.e., the Cu atoms are isolated from each other by the silica matrix and no Cu NPs are formed. The corresponding absorption spectrum in the as-implanted state (curve (i) in Fig. 1(b)) shows very faint absorption in the Vis-NIR regions. A naked eye investigation did not observe any color in the sample as shown in Fig. 1(c-i). Since the SPR absorption around 2 eV is a consequence of aggregation of Cu atoms, the faint absorption in the Vis region is consistent with the EXAFS result.

After the implantations, the samples were annealed at 650 °C for 1 h in flowing forming gas (5%– H_2 + 95%– N_2) to induce precipitation and growth of Cu NPs. The sample color changed from transparent to reddish brown (Fig. 1(c-ii)). As shown in Fig. 1(a), the 1.45 Å peak ascribed to isolated Cu atoms disappears and the 2.2 Å peak ascribed to the Cu–Cu nearest-neighbor (NN) shell has the strongest intensity. In addition, several peaks due to the next NN and higher order shells are observed at the longer distance side of the strongest peak. These features, including the peak intensity ratios between the higher order shells, are comparable to a bulk Cu standard, confirming the formation of *crystalline* Cu NPs. The corresponding optical absorption (curve (ii) in Fig. 1(b)) gradually increases with the photon energy with a broad SPR peak around 2.2 eV. Similar spectra have been reported extensively in past literature.^{1,10–12}

After the annealing, the samples were irradiated with Sn^{3+} ions of 5 MeV up to a fluence of 1×10^{14} ions/cm² at LNT. The intensity of the NN Cu–Cu peak decreases as shown in Fig. 1(a). While the peaks of the higher order shells are very weak but faintly visible, the intensity ratios between the peaks are completely different from those of the crystalline NPs. These features are consistent with the past literature of the amorphization of thin Co films⁶ and of other alloy systems.¹³

After irradiation, the sample clearly changed color from reddish brown to dark brown (Fig. 1(c-iii)). The corresponding absorption spectrum is shown in Fig. 1(b). However, it should be noted that the observed spectrum might consist of not only the contribution of the amorphous Cu NPs but also those of others, i.e., radiation damage and dispersed Cu atoms.

Since the ion range of the 5 MeV Sn ions is much deeper than 2 μm , i.e., far beyond the NP layer (0.6–1.0 μm in depth), impurity effects of Sn ions in Cu NPs are negligible. For reference, a piece of virgin silica was irradiated by the Sn ions of the same energy and fluence. The absorption spectrum (curve (iv) in Fig. 1(b)) shows almost no absorption up to 4 eV but an absorption peak at around 5 eV. This is a typical absorption band of radiation-induced defects in the KU-1 type silica.^{14,15}

In the spectrum of Sn-irradiated Cu NPs (curve (iii) in Fig. 1(b)), the same peak as described above was observed. To eliminate the contribution of such radiation-induced defects, curve (iv) was subtracted from curve (iii). After the subtraction, a smooth spectrum (not shown) was obtained in whole the UV region, which justifies this subtraction procedure.

As shown in Fig. 1(a), the Sn irradiation induced re-appearance of the peak at 1.45 Å, from collision-induced dissolution of Cu NPs. The dissolution of metal NPs induced by irradiation of several MeV heavy ions is a relatively common phenomenon reported previously.^{16,17} From Fig. 1(a), it was estimated that 40 at. % of Cu existed as dispersed atoms and the remaining 60 at. % formed the NPs.⁷ In order to study the NP absorption profile only, curve (i) (weighted at 40%) was subtracted from curve (iii). The resulting absorption spectrum of amorphous Cu NPs is shown in Fig. 2(a) together with the spectrum of crystalline NPs before irradiation. For comparison, the spectra were normalized with the Cu content which forms NPs.

From SAXS measurements, the volume-weighted mean diameters were determined as 2.5 ± 0.1 nm and 2.7 ± 0.1 nm before and after the amorphization, respectively, indicating almost the same mean size (and size distribution).⁷ The electron mean-free-path (EMFP) l in crystalline Cu NPs of radius r is given

$$l^{-1} = l_{\infty}^{-1} + \frac{A}{r}. \quad (1)$$

where l_{∞} and A denote the EMFP of bulk Cu of 42 nm and a constant of ~ 1 , respectively.¹⁸ Assuming $A = 1$, the EMFP of *crystalline* Cu NPs of 2.5 nm in diameter was estimated as 1.2 nm. Much reduced EMFPs in NPs comparing with the

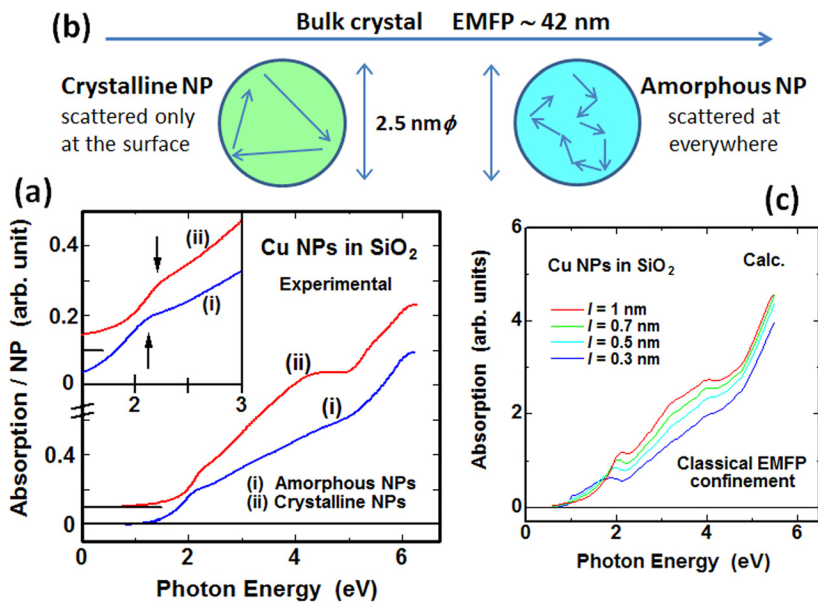


FIG. 2. (Color online) (a) Optical absorption spectrum of amorphous Cu NPs in silica as determined from a spectrum of Cu NPs irradiated with 5 MeV Sn^{3+} ions by subtracting the contributions of dispersed Cu atoms and radiation-induced defects in silica. The corresponding spectrum of *crystalline* Cu NPs of the same mean size and size distribution is also shown. The upper-left inset shows the expanded spectra around the surface plasmon resonance. (b) Schematically depicted EMFP in bulk crystal, crystalline NPs of 2.5 nm in diameter, and amorphous NPs of the same diameter. (c) Calculated spectra of Cu NPs in silica with four different EMFP l . Although the dielectric function of crystalline Cu was used, the spectra can be applicable to the amorphous Cu NPs with adjusting the EMFP. It should be noted that crystalline NPs with the diameter of 2.5 nm have the EMFP of 1.2 nm.

bulk are schematically shown in Fig. 2(b). Upon amorphization, the low-energy SPR peak (at around 2.2 eV) showed a small but certain shift and the absorption structure around 4 eV became less prominent (see Fig. 2(a)).

The EMFP dependence of the absorption spectra of Cu NPs in silica was calculated based on the classical size effect (an EMFP reduction¹⁸) and is shown in Fig. 2(c). The complex dielectric function of Cu NPs $\varepsilon(\omega)$ was given as a sum of the interband part $\varepsilon_b(\omega)$ and the free electron part described by the Drude formula $\varepsilon_{\text{Drude}}(\omega)$

$$\varepsilon(\omega) = \varepsilon_{\text{Drude}}(\omega) + \varepsilon_b(\omega) = 1 - \frac{\omega_p^2}{\omega^2 + i\omega/\tau} + \varepsilon_b(\omega). \quad (2)$$

where $\hbar\omega_p$ and τ denote the bulk plasmon energy of 8.86 eV and the relaxation time. The relaxation time τ changes with the EMFP l keeping the relation $\tau = l/v_F$, where v_F denotes the Fermi velocity of Cu. The absorption spectra were calculated by the Maxwell-Garnett theory.¹⁹ See Ref. 9 for details.

The calculation well reproduced that with decreasing the EMFP, there were (I) a low-energy shift of the SPR and (II) less prominence of the 4 eV structure. Both the spectral features of the amorphous Cu NPs were explained by strongly reduced EMFP, in spite of the NP size remaining virtually unchanged upon amorphization.

These observations indicate that the EMFP of amorphous Cu NPs is clearly shorter than the crystalline value of 1.2 nm. On the other hand, Ioffe and Regel²⁰ assumed that the EMFP of amorphous materials should be the same as or greater than the inter-atomic distance, which was determined as 0.22 nm from the EXAFS data shown in Fig. 1(a). Consequently, the range of the EMFP in the amorphous Cu NPs was estimated as

$$0.22 \text{ nm} \leq \text{EMFP}(\text{amorphous Cu NPs}) \ll 1.2 \text{ nm}. \quad (3)$$

In conclusion, we have presented optical absorption spectra of crystalline and amorphous Cu NPs embedded in silica. While the NP size remained virtually unchanged upon

amorphization, it was found that the EMFP was significantly reduced. This can be explained by the increased number of scattering sites due to the loss of lattice periodicity.

Part of this research was undertaken on the XAS beamline at the Australian Synchrotron, Victoria, Australia.

- ¹R. F. Haglund, L. Yang, R. H. Magruder, C. W. White, R. A. Zuhr, L. Yang, R. Dorsinville, and R. R. Alfano, *Nucl. Instrum. Methods Phys. Res. B* **91**, 493 (1994).
- ²S. Nie and S. R. Emory, *Science* **275**, 1102 (1997).
- ³H. A. Atwater, S. Majer, A. Polman, J. A. Dionne, and L. Sweatlock, *MRS Bull.* **30**, 385 (2005).
- ⁴W. A. Harrison, *Electronic Structure and the Properties of Solids—The Physics of the Chemical Bond* (Dover, New York, 1980).
- ⁵K. S. Suslick, S.-B. Choe, A. A. Cichowlas, and M. W. Grinstaff, *Nature* **353**, 414 (1991).
- ⁶H. Mangan, D. Chandris, G. Rossi, G. Jezequel, K. Hricovini, and J. Lecante, *Phys. Rev. B* **40**, 9989 (1989).
- ⁷B. Johannessen, P. Kluth, D. J. Llewellyn, G. J. Foran, D. J. Cookson, and M. C. Ridgway, *Phys. Rev. B* **76**, 184203 (2007).
- ⁸D. J. Sprouster, R. Giulian, L. L. Araujo, P. Kluth, B. Johannessen, N. Kirby, K. Nordlund, and M. C. Ridgway, *Phys. Rev. B* **81**, 155414 (2010).
- ⁹H. Amekura, Y. Takeda, and N. Kishimoto, *Nucl. Instrum. Methods Phys. Res. B* **222**, 96 (2004).
- ¹⁰R. H. Magruder III, R. A. Weeks, R. A. Zuhr, and G. Whichard, *J. Non-Cryst. Solids* **129**, 46 (1991).
- ¹¹N. Kishimoto, V. T. Gritsyna, K. Kono, H. Amekura, and T. Saito, *Nucl. Instrum. Methods Phys. Res. B* **127–128**, 579 (1997).
- ¹²E. Cattaruzza, G. Battaglin, F. Gonella, R. Polloni, G. Mattei, C. Maurizio, P. Mazzoldi, C. Sada, M. Montagna, C. Tosello, and M. Ferrari, *Philos. Mag.* **B 82**, 735 (2002).
- ¹³A. Sadoc, D. Raoux, P. Lagarde, and A. Fontaine, *J. Non-Cryst. Solids* **50**, 331 (1982).
- ¹⁴H. Amekura and N. Kishimoto, *J. Appl. Phys.* **104**, 063509 (2008).
- ¹⁵H. Amekura, N. Ishikawa, N. Okubo, M. C. Ridgway, R. Giulian, K. Mitsuishi, Y. Nakayama, C. Buchal, S. Mantl, and N. Kishimoto, *Phys. Rev. B* **83**, 205401 (2011).
- ¹⁶G. Rizza, H. Cheverry, T. Gacoin, A. Lamasson, and S. Henry, *J. Appl. Phys.* **101**, 014321 (2007).
- ¹⁷K.-H. Heinig, T. Mueller, B. Schmidt, M. Strobel, and W. Moeller, *Appl. Phys. A* **77**, 17 (2003).
- ¹⁸U. Kreibitz and M. Vollmer, *Optical Properties of Metal Clusters* (Springer, Berlin, 1995).
- ¹⁹J. C. Maxwell-Garnett, *Philos. Trans. R. Soc. London, Ser. A* **203**, 385 (1904).
- ²⁰N. Mott, *Conduction in Non-crystalline Materials* (Oxford University Press, Oxford, 1987).